Xi'an Shiyou Daxue Xuebao (Ziran Kexue Ban)/
Journal of Xi'an Shiyou University, Natural Sciences Edition
ISSN: 1673-064X
E-Publication: Online Open Access
Vol: 67 Issue 09 | 2024
DOI: 10.5281/zenodo.13740609

CHARACTERIZATION OF SECONDARY VORTEX THROUGH 90-DEGREE PIPE BEND OF DIFFERENT CROSS SECTIONS AND CURVATURE RATIOS

UMAIR MUNIR *
Mechanical Engineering Department, NFC IEFR, Faisalabad, Pakistan.
*Corresponding Author Email: umair.munir1@gmail.com

SYED MURAWAT ABBAS NAQVI
Mechanical Engineering Department, NFC IEFR, Faisalabad, Pakistan.

MUHAMMAD YASAR JAVAID
Department of Mechanical Engineering Technology, Government College University, Faisalabad, Pakistan.

MUHAMMAD WAQAS
Department of Mechanical, Industrial and Energy Systems, College of Engineering and Technology, University of Sargodha, Sargodha, Pakistan.

HAFIZ MUHAMMAD WAQAS
Mechanical Engineering Department, NFC IEFR, Faisalabad, Pakistan.

Abstract

Bends are primary source of formation of secondary flow and swirling vortices in pipes, channels and ducts. Flow losses and heat transfer are strongly affected by presence of bends in the flow passage therefore, in depth characterization of flow through bends is required. In the current study, the three dimensional, turbulent and incompressible flow through 90-degree bend is examined by using a CFD package Star CCM+. The data is analyzed in the results section to evaluate the effect of changing bend curvature ratio *($\lambda=R_C/d$)* and shape of cross section on intensity of secondary flow. It is observed that swirl intensity reduces drastically as curvature ratio is increased. Twin secondary vortices are formed and their intensity is a function of pressure gradient in the curved region of bend. Furthermore, it is found that circular cross section better supports the formation of dean vortices and secondary flow as compared to square and rectangular cross sections. The intensity of swirling vortices is also found decreasing as the aspect ratio of the rectangular section is increased up to 3:1. It means that there are lower flow losses for rectangular cross section bends with high aspect ratios as compared to square and circular cross section bends.

Index Terms: Dean Vortices, Secondary Flow, 90^o Pipe Bend, Swirl Intensity, Pressure Coefficient.

1. INTRODUCTION

Pipe bends are essential and key component of any piping system which are primarily used to divert the flow direction [1]. They are used in infrastructure for heating, ventilation and air conditioning (HVAC) system, plumbing and fire protection systems. Industries like pharmaceutical, petrochemical, beverages, power production and chemical processing are majorly relying on the design of their piping system for transportation of liquids, slurries, and gases [2]. The optimized design of piping system is accomplished by carefully selecting the suitable bends, fitting and valves for minimum losses [3].

Xi'an Shiyou Daxue Xuebao (Ziran Kexue Ban)/
Journal of Xi'an Shiyou University, Natural Sciences Edition
ISSN: 1673-064X
E-Publication: Online Open Access
Vol: 67 Issue 09 | 2024
DOI: 10.5281/zenodo.13740609

The flow physics associated with pipe bends is investigated by many researchers by using experimental [4]and numerical methods [5], [6], [7]. The unsteadiness in flow through a bend is a function of Reynold's Number (Re) and pipe bend curvature radius. As the fluid passes through a curved section of pipe, a pressure gradient is formed having low pressure at the inner surface and high pressure at the outer surface. This is due to the action of centrifugal force on fluid particle moving in a curved path [8]. This pressure gradient causes the formation of secondary flow and dean vortices, which is a pair of counter rotating vortex [9]. The secondary flow is formed due to movement of fluid particles perpendicular to primary flow direction. Adverse pressure gradients are observed for small bend curvature radius *($\lambda \leq 1.5$)* causing high flow losses [10]. Along with secondary flow and formation of dean vortices due to bends, flow separation is another phenomenon that occurs due to bends. Dutta et al. [11] investigated the flow separation in 90- degree bends in and found that the flow separation is significant for bends having low curvature radius. The erosion of pipe bends due to presence of particles and methods to reduce them are suggested by many researchers[12], [13]. The strength of secondary flow can be reduced by introducing a W-Weir at the end of bend section [14]. Another phenomenon that is associated with bends in accumulation and deposition of particles over time [15], [16].

Heat transfer from heat sinks is improved by introducing sinusoidal channels that causes secondary flow and hence improve fluid mixing [17], [18], [19]. Bends are also involved in many tubular heat exchangers [20]. Cooling of internal combustion engine is improved by vorticity of flow caused by 90-degree bend [21].

The measurement of flow losses and associated intensity of secondary flow is critical in most of the incompressible flow system. The flow physics of turbulent, incompressible flow at downstream of a 90-degree bend is not fully clarified yet. The effect of cross section changes on intensity of dean vortices require investigation. Therefore, this work is aimed to analyze the flow physics through 90-degree bend to see the effect of bend curvature ratio and change of cross section on characteristics of secondary flow.

2. PHYSICAL MODEL AND PROBLEM DESCRIPTION

2.1 Governing equations and mathematical model

The problem described above is a 3-dimentional, turbulent, incompressible in a steady state. Therefore, the numerical model for the current model consists of one equation of continuity and three equations of momentum given by Eq. **(1)** and **(2)** respectively. In addition to these conservation equations, the mathematical model also includes two equations of ($k-\omega$) turbulence model.

$$\nabla.(\rho\vec{V}) = 0 \qquad \textbf{(1)}$$

$$\nabla\left[\vec{V}.(\rho\vec{V})\right] = -\nabla p - \frac{2}{3}\nabla\left[\mu(\nabla.\vec{V})\right] + \nabla.\left[\mu(\nabla\vec{V})^{T}\right] + \nabla.\left[\mu(\nabla\vec{V})\right] \qquad \textbf{(2)}$$

Xi'an Shiyou Daxue Xuebao (Ziran Kexue Ban)/
Journal of Xi'an Shiyou University, Natural Sciences Edition
ISSN: 1673-064X
E-Publication: Online Open Access
Vol: 67 Issue 09 | 2024
DOI: 10.5281/zenodo.13740609

2.2 Problem description

Fig 1 shows the computational domain of the problem having a bend curvature ratio of $R_C/d=2$ where d is the pipe diameter. The working fluid was air having density of 1.225 kg/m^3. The upstream and downstream lengths are 20d and 50d respectively in order to achieve fully developed flow conditions. The upstream and downstream pipe length are normalized as y/d and x/d respectively.

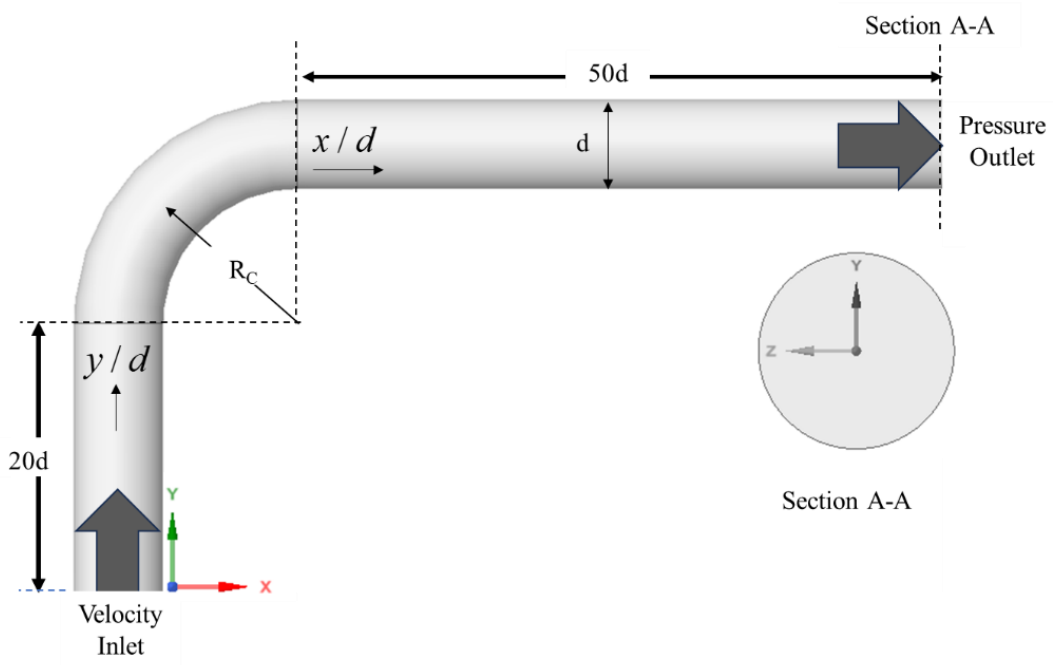

Fig 1: 90-degree pipe bend with upstream and downstream lengths

Three dimensional polyhedral elements are used for meshing with prism layers. Built in mesher of Star CCM software is used to develop three different mesh sizes having 276190, 441,317 and 1,167,240 elements to obtain an optimized solution via grid independence study.

The Reynold's number corresponding to inlet velocity is 60,000 to match the experimental conditions of Kim et al. [22], Sudo et al. [23]and Tanaka et al. [24] by using air as working fluid.

2.3 Model validation

For validation, the axial velocity at bend outlet was normalized with the inlet velocity and plotted in Fig 2 for comparison with the data presented by Kim et al. [22], Sudo et al. [23] and Tanaka et al. [24]. The geometric and boundary conditions are matched with above mentioned references having $\lambda=2$ and $Re=60,000$. The fine mesh with 1.16 million cells is used for simulation having polyhedral cells.

Xi'an Shiyou Daxue Xuebao (Ziran Kexue Ban)/
Journal of Xi'an Shiyou University, Natural Sciences Edition
ISSN: 1673-064X
E-Publication: Online Open Access
Vol: 67 Issue 09 | 2024
DOI: 10.5281/zenodo.13740609

The normalized velocity *u*(x)* given by Eq. **(1)** is obtained at the bend outlet. Where *u* is the x-component of velocity at bend outlet and U_b is the inlet velocity. A close agreement is observed between the normalized velocity profiles hence, fine mesh with 1.16 million cells is used for further analysis.

$$u^*(x) = \frac{u}{U_b} \qquad (3)$$

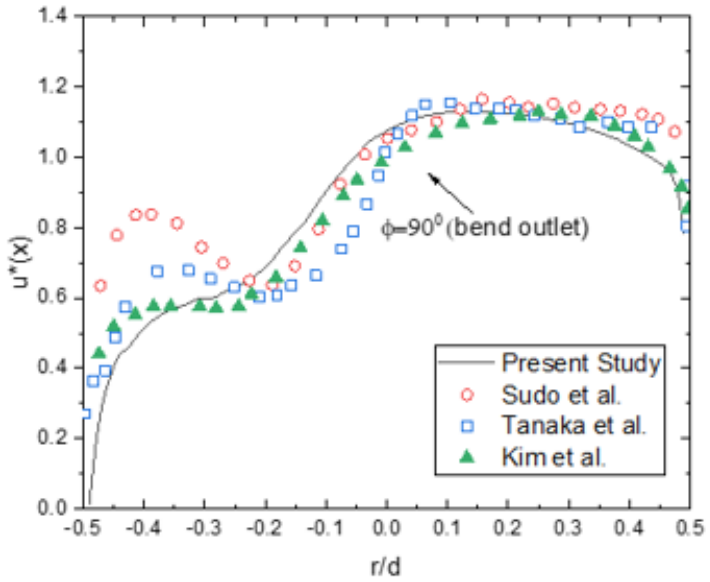

Fig 2: Normalized axial velocity profile at 90-degree bend outlet

3. RESULTS AND DISCUSSION

In this work, the effect of bend curvature and change of cross section is investigated in different subsections on normalized velocity profile, swirl intensity and pressure coefficient. All other boundary conditions at inlet and outlet remain unchanged in the analysis.

3.1 Bend curvature ratio effects

The velocity variation at the 90-degree bend outlet is presented in Fig 3 at four different curvature ratios. The negative radial distance is representing the inner region of the bend. The highest velocity gradients are observed in the inner region for bend curvature ratio of *λ=1.* The velocity profiles get smoother as the bend curvature ratio is increased.

Xi'an Shiyou Daxue Xuebao (Ziran Kexue Ban)/
Journal of Xi'an Shiyou University, Natural Sciences Edition
ISSN: 1673-064X
E-Publication: Online Open Access
Vol: 67 Issue 09 | 2024
DOI: 10.5281/zenodo.13740609

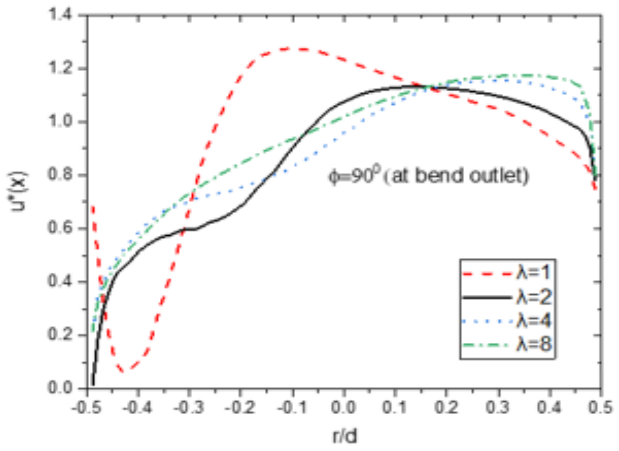

Fig 3: Axial velocity profile for 90-degree bend at different curvature ratios

The swirl intensity of the dean vortices is estimated at the bend outlet by using Eq. (4) and plotted in Fig **4**. Where *v* and *w* are velocity components normal to primary flow direction in *y* and *z* direction respectively and U_b is the velocity at inlet.

$$I_s = \frac{\int (v^2 + w^2) dA}{U_b^2 \int dA} \qquad \textbf{(4)}$$

The intensity of dean vortices is significantly affected by radius of bend as evident from Fig **4**. The swirl intensity is dropped drastically when the curvature ratio λ is increased from 1 to 2. It is also observed that the intensity of dean vortices is almost diminished at *20d* downstream of bend for all four cases under investigation.

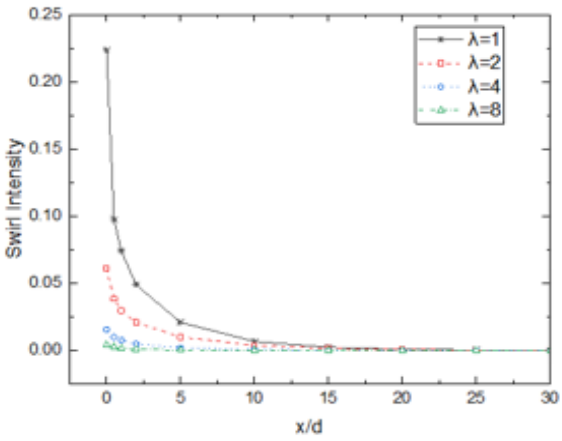

Fig 4: Swirl Intensity at downstream of 90-degree bend at different bend curvatures

Xi'an Shiyou Daxue Xuebao (Ziran Kexue Ban)/
Journal of Xi'an Shiyou University, Natural Sciences Edition
ISSN: 1673-064X
E-Publication: Online Open Access
Vol: 67 Issue 09 | 2024
DOI: 10.5281/zenodo.13740609

The pressure coefficient is defined by to Eq. **(5)** where p is the termed as static pressure, p_{ref} is the reference pressure at inlet, ρ is density of air and U_b is the inlet velocity.

$$C_p = \frac{p - p_{ref}}{0.5\rho U_b^{\,2}} \qquad \textbf{(5)}$$

The pressure coefficient computed from Eq. **(5)** in the dimensionless form for different curvature ratios is presented in **Fig 5(a)**. The curvature ratio is significantly affecting the pressure gradients as highest-pressure gradient is observed for the sharp bend having curvature ratio of *λ=1.* The higher-pressure gradients cause stronger secondary flow with high swirl intensity dean vortices: hence, results higher turbulence and high-pressure loss.

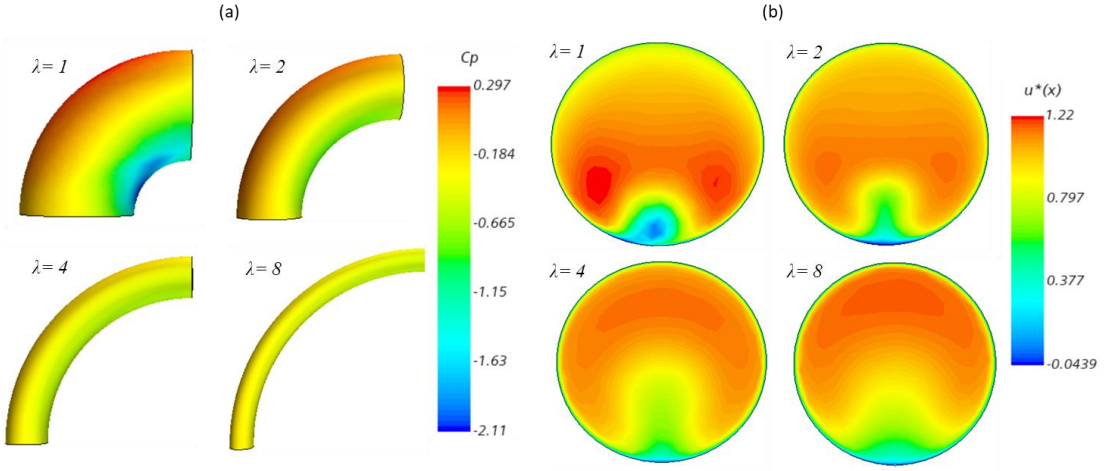

Fig 5: (a)Pressure coefficient (b)Normalized velocity contours at different bend curvature ratios

3.2 Effect of change of pipe cross-section

In this section, four different cross sections are compared to see the effect of change of cross section on the velocity profile, pressure coefficient and swirl intensity. The cross sections used in the analysis are circular, square, and two rectangular cross sections having 2:1 and 3:1 aspect ratio. The bend curvature ratio and Reynold's number are kept contact i.e. λ =2 and Re=60,000 for all four cases under investigation.

Fig 6 presents the axial velocity profiles at the bend outlet for different cross sections. It is evident that change of cross section is significantly affecting the axial velocity profile at the bend outlet. The velocity profile for circular had the highest velocity variations and flatness of the velocity profiles increases as the aspect ratio for square and rectangular cross section is increased. This is due to the fact that fluid velocity components in the secondary flow which are in normal direction to primary are rapidly diminished at flat wall surfaces as compared to circular wall surface. Therefore, decreasing the level of

Xi'an Shiyou Daxue Xuebao (Ziran Kexue Ban)/
Journal of Xi'an Shiyou University, Natural Sciences Edition
ISSN: 1673-064X
E-Publication: Online Open Access
Vol: 67 Issue 09 | 2024
DOI: 10.5281/zenodo.13740609

turbulence and low intensity vortices are formed for square and rectangular cross sections.

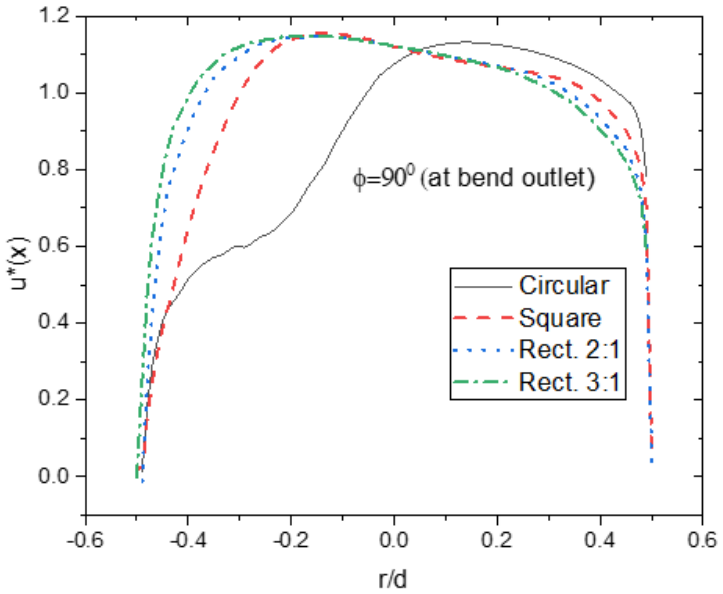

Fig 6: Axial velocity profile for 90-degree bend at pipe/duct cross sections

Fig 7(a) presents the pressure coefficient contours at 90-degree bend for different cross section shapes by keeping other boundary conditions unchanged. The extreme pressure gradient is observed for square and circular cross sections followed by rectangular cross sections.

Fig 7(b) is presenting normalized axial velocity contour lines showing two counter rotating vortices at the bend at the bend outlet. A similar pattern can be observed that the size and severity of dean vortices is lowered for rectangular cross sections which is further reduced as the aspect ratio is increased.

The swirl intensity is the measure of turbulence and indicate the severity of secondary flow. Fig 8 shows the intensity of the twin vortices at bend outlet for different cross sections and its dissipation rate at the downstream section.

Although the pressure gradient was highest for square cross section, but the swirl intensity for circular is found maximum. That means circular cross section provide better mixing by formation of strong vortices as evident from Fig 7(b). Whereas, the lowest swirl intensity is observed for rectangular cross with aspect ratio of 3:1.

Xi'an Shiyou Daxue Xuebao (Ziran Kexue Ban)/
Journal of Xi'an Shiyou University, Natural Sciences Edition
ISSN: 1673-064X
E-Publication: Online Open Access
Vol: 67 Issue 09 | 2024
DOI: 10.5281/zenodo.13740609

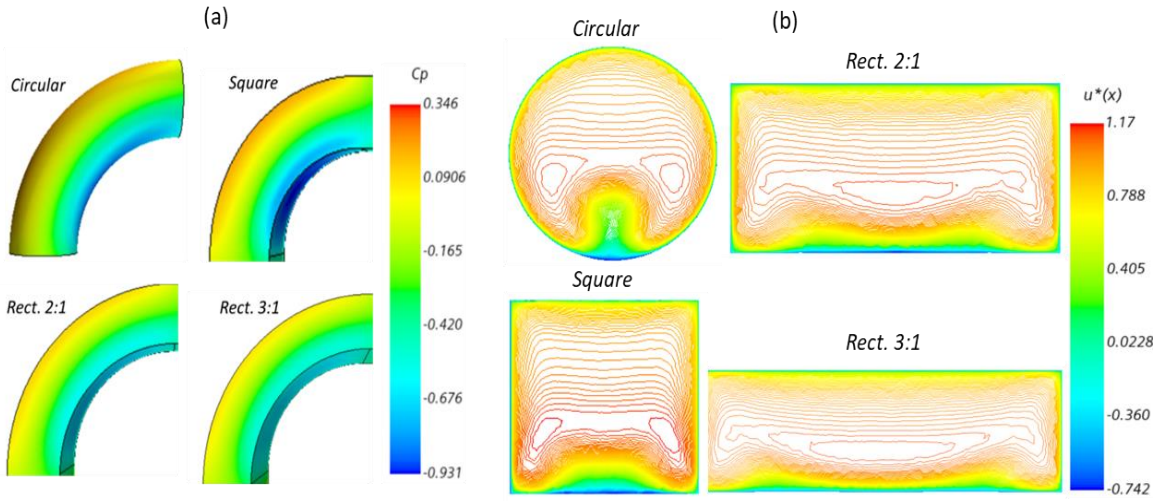

Fig 7: (a)Pressure coefficient (b)Normalized velocity contours at different cross sections

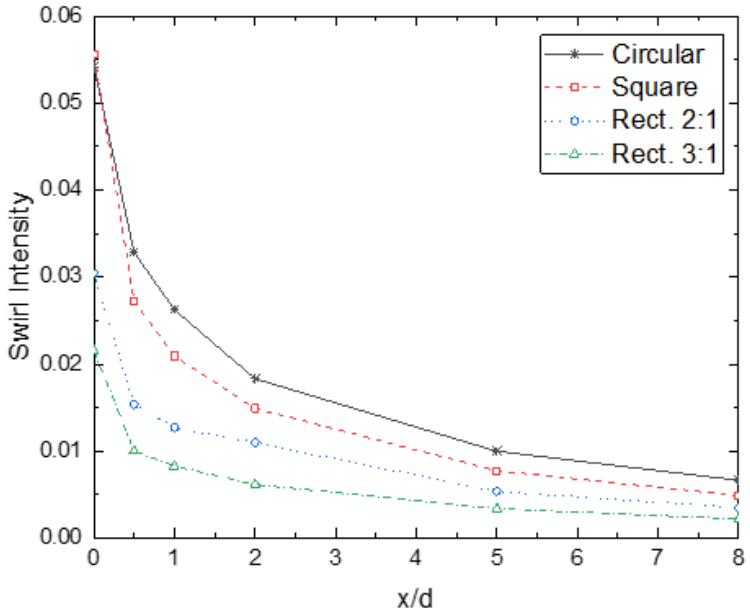

Fig 8: Swirl Intensity at downstream of 90-degree bend at different cross sections

4. CONCLUSIONS

Incompressible, steady, three dimensional, and turbulent flow through 90-degree bend is analyzed in the current study. The work is aimed to investigate the effect of cross section change and bend curvature ratio on the characteristics of secondary flow and dean vortices at constant Reynold's number.

Xi'an Shiyou Daxue Xuebao (Ziran Kexue Ban)/
Journal of Xi'an Shiyou University, Natural Sciences Edition
ISSN: 1673-064X
E-Publication: Online Open Access
Vol: 67 Issue 09 | 2024
DOI: 10.5281/zenodo.13740609

The major findings of this work are stated as under:

- The gradient of pressure coefficient at the bend section is a strong function of bend curvature ratio *(λ).* Sharp bends causes most adverse pressure gradients due to deceleration of flow at the inner region and acceleration of flow in the outer bend region. The severe pressure gradient results in high intensity swirls formation called secondary flow. It is observed that intensity of swirls is significantly dropped as the bend curvature ratio *(λ)* is increased from 1 to 2.
- The shape of cross section is strongly affecting the characteristics of secondary flow at constant hydraulic diameter, bend curvature ratio and Reynold's number. The maximum pressure gradient is observed for square cross section followed by circular and then rectangular cross sections. In response to that, the intensity of swirls was maximum for circular cross section followed by square and rectangular cross sections. It means that the flat surfaces of square and rectangular cross sections are damping the intensity of secondary flow. Furthermore, it is found that swirl intensity is further reduced as the aspect ratio of rectangular cross section is increased from 2:1 to 3:1.

The inclusion of bends in the flow path cause formation of dean vortices that can enhance heat transfer through better mixing. Additional studies are required in future to see the effect of bends in channel and tube for improved thermal performance.

Nomenclature

C_p	Pressure coefficient, [-]	*Re*	Reynold's Number [-]
d	Pipe diameter, [m]	U_b	Inlet velocity, [m sec^{-1}]
I_s	Swirl Intensity, [-]	*u*(x)*	Normalized axial velocity, [-]
p	Static pressure, [Pa]	*v,w*	Velocity in *y* and *z* direction, [m sec^{-1}]
p_{ref}	Pressure at inlet, [Pa]	*λ*	Bend curvature ratio, [-]

References

1) M. Ayala and J. M. Cimbala, "Numerical approach for prediction of turbulent flow resistance coefficient of 90° pipe bends," Proceedings of the Institution of Mechanical Engineers, Part E: Journal of Process Mechanical Engineering, vol. 235, no. 2, 2021, doi: 10.1177/0954408920964008.

2) J. P. Singh, S. Kumar, and S. K. Mohapatra, "Simulation and optimization of coal-water slurry suspension flow through 90° pipe bend using CFD," International Journal of Coal Preparation and Utilization, vol. 41, no. 6, 2021, doi: 10.1080/19392699.2018.1488693.

3) S. Kumar, M. Kumar, S. Samanta, M. Ukamanal, A. R. Pradhan, and S. B. Prasad, "Simulations of water flow in a horizontal and 900 pipe bend," Mater Today Proc, vol. 56, 2022, doi: 10.1016/j.matpr.2022.02.528.

4) P. Vollestad, L. Angheluta, and A. Jensen, "Experimental study of secondary flows above rough and flat interfaces in horizontal gas-liquid pipe flow," International Journal of Multiphase Flow, vol. 125, 2020, doi: 10.1016/j.ijmultiphaseflow.2020.103235.

5) J. Zhang, D. Wang, W. Wang, and Z. Zhu, "Numerical Investigation and Optimization of the Flow Characteristics of Bend Pipe with Different Bending Angles," Processes, vol. 10, no. 8, 2022, doi: 10.3390/pr10081510.

ISSN: 1673-064X
E-Publication: Online Open Access
Vol: 67 Issue 09 | 2024
DOI: 10.5281/zenodo.13740609

6) L. Tang, S. Yuan, M. Malin, and S. Parameswaran, “Secondary vortex-based analysis of flow characteristics and pressure drop in helically coiled pipe,” Advances in Mechanical Engineering, vol. 9, no. 4, 2017, doi: 10.1177/1687814017700059.

7) R. Wu and L. Qin, “Numerical Study on Flow Characteristics and Energy Loss Mechanism in the 90° Circular Pipe Bend,” in Proceedings - 2019 International Conference on Advances in Construction Machinery and Vehicle Engineering, ICACMVE 2019, 2019. doi: 10.1109/ICACMVE.2019.00083.

8) Y. Liu, T. Stoesser, and H. Fang, “Effect of secondary currents on the flow and turbulence in partially filled pipes,” J Fluid Mech, vol. 938, 2022, doi: 10.1017/jfm.2022.141.

9) K. G. Bilde, K. Sørensen, and J. Hærvig, “Decay of secondary motion downstream bends in turbulent pipe flows,” Physics of Fluids, vol. 35, no. 1, 2023, doi: 10.1063/5.0129339.

10) Seroor Atalah Khaleefa Ali, “Study of Pressure Losses in Piping System,” International Journal of Science and Research, vol. 8, no. 6, 2019.

11) P. Dutta, S. K. Saha, N. Nandi, and N. Pal, “Numerical study on flow separation in 90° pipe bend under high Reynolds number by k-ε modelling,” Engineering Science and Technology, an International Journal, vol. 19, no. 2, 2016, doi: 10.1016/j.jestch.2015.12.005.

12) R. Li, Z. Sun, A. Li, Y. Li, and Z. Wang, “Design optimization of hemispherical protrusion for mitigating elbow erosion via CFD-DPM,” Powder Technol, vol. 398, 2022, doi: 10.1016/j.powtec.2022.117128.

13) A. Kosinska, B. V. Balakin, and P. Kosinski, “Theoretical analysis of erosion in elbows due to flows with nano- and micro-size particles,” Powder Technol, vol. 364, 2020, doi: 10.1016/j.powtec.2020.02.002.

14) V. Atashi, M. S. Bejestan, and Y. H. Lim, “Flow Pattern and Erosion in a 90-Degrees Sharp Bend around a W−Weir,” Water (Switzerland), vol. 15, no. 1, 2023, doi: 10.3390/w15010011.

15) A. Ladino, C. A. Duque-Daza, and S. Lain, “Effect of walls with large scale roughness in deposition efficiency for 90-degree square bend configurations,” J Aerosol Sci, vol. 167, 2023, doi: 10.1016/j.jaerosci.2022.106093.

16) Y. Yan, Y. Zhao, J. Yao, and C. H. Wang, “Investigation of particle transport by a turbulent flow through a 90° bend pipe with electrostatic effects,” Powder Technol, vol. 394, 2021, doi: 10.1016/j.powtec.2021.08.066.

17) X. Liu, Y. Fu, J. Wang, and J. Ge, “Dean instability and thermal characteristic in sinusoidal structure,” Int J Heat Mass Transf, vol. 206, 2023, doi: 10.1016/j.ijheatmasstransfer.2023.123938.

18) X. Liu, Y. Fu, J. Wang, H. Zhang, and J. Zhu, “Investigation on flow and heat transfer in rectangular cross-section sinusoidal channels,” International Journal of Thermal Sciences, vol. 176, 2022, doi: 10.1016/j.ijthermalsci.2022.107490.

19) S. L. Wang et al., “Heat transfer enhancement of symmetric and parallel wavy microchannel heat sinks with secondary branch design,” International Journal of Thermal Sciences, vol. 171, 2022, doi: 10.1016/j.ijthermalsci.2021.107229.

20) H. Bin Zahid, A. Mubashar, M. Waqas, M. H. Siddiqi, U. Munir, and S. M. A. Naqvi, “Experimental and Cfd Simulation Study of Shell and Tube Heat Exchangers with Different Baffle Segment Configurations,” Thermal Science, vol. 27, no. 1, 2023, doi: 10.2298/TSCI220124075Z.

21) S. Wegt, R. Maduta, J. Kissing, J. Hussong, and S. Jakirlić, “LES-based vortical flow characterization in a 90°-turned pipe bend,” Comput Fluids, vol. 240, 2022, doi: 10.1016/j.compfluid.2022.105418.

ISSN: 1673-064X
E-Publication: Online Open Access
Vol: 67 Issue 09 | 2024
DOI: 10.5281/zenodo.13740609

22) J. Kim, M. Yadav, and S. Kim, “Characteristics of secondary flow induced by 90-degree elbow in turbulent pipe flow,” Engineering Applications of Computational Fluid Mechanics, vol. 8, no. 2, 2014, doi: 10.1080/19942060.2014.11015509.

23) K. Sudo, M. Sumida, and H. Hibara, “Experimental investigation on turbulent flow in a circular-sectioned 90-degree bend,” Exp Fluids, vol. 25, no. 1, pp. 42–49, 1998, doi: 10.1007/S003480050206/METRICS.

24) M. A. Tanaka, H. Ohshima, and H. Monji, “Numerical investigation of flow structure in pipe elbow with large Eddy simulation approach,” in American Society of Mechanical Engineers, Pressure Vessels and Piping Division (Publication) PVP, 2010. doi: 10.1115/PVP2009-77598.